DEVELOPMENT OF UNSTEADY AERODYNAMIC AND AEROELASTIC REDUCED-ORDER MODELS USING THE FUN3D CODE

Walter A. Silva[1], Veer N. Vatsa[2], and Robert T. Biedron[2]

[1]Aeroelasticity Branch
Walter.A.Silva@nasa.gov

[2]Computational Aerosciences Branch
NASA Langley Research Center
Hampton, Virginia 23681-0001

Keywords. FUN3D, ROM, aeroelasticity, flutter, root locus.

Abstract. Recent significant improvements to the development of CFD-based unsteady aerodynamic reduced-order models (ROMs) are implemented into the FUN3D unstructured flow solver. These improvements include the simultaneous excitation of the structural modes of the CFD-based unsteady aerodynamic system via a single CFD solution, minimization of the error between the full CFD and the ROM unsteady aerodynamic solution, and computation of a root locus plot of the aeroelastic ROM. Results are presented for a viscous version of the two-dimensional Benchmark Active Controls Technology (BACT) model and an inviscid version of the AGARD 445.6 aeroelastic wing using the FUN3D code.

1 INTRODUCTION

The goal behind the development of reduced-order models (ROMs) for the rapid computation of unsteady aerodynamic and aeroelastic responses is aimed at addressing two challenges. The first challenge is the computational cost associated with full CFD aeroelastic simulations, which increases with the fidelity of the nonlinear aerodynamic equations to be solved as well as the complexity of the configuration. Computational cost, however, may be reduced via the implementation of parallel processing techniques, advanced algorithms, and improved computer hardware processing speeds.

The second, more serious, challenge is that the information generated by these simulations cannot be used effectively within a preliminary design environment. Because the output of these full CFD aeroelastic simulations cannot be incorporated within a design environment, parametric variations and design studies can only be performed by trial-and-error. As a result, the integration of traditional, computational aeroelastic simulations into preliminary design activities involving disciplines such as aeroelasticity, aeroservoelasticity (ASE), and optimization is, at present, a costly and impractical venture.

Development of a ROM entails the development of a simplified mathematical model that captures the dominant dynamics of the original system. This alternative mathematical representation of the original system is, by design, in a mathematical form suitable for use in a multidisciplinary, preliminary design environment. As a result, interconnection of the ROM with other disciplines is possible, thereby addressing the second challenge. The simplicity of the ROM yields significant improvements in computational efficiency as compared to the original system, thereby addressing the first challenge.

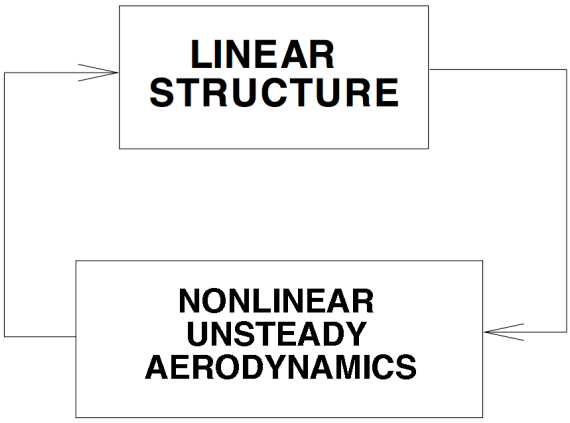

Figure 1: Coupling of linear structural model and nonlinear unsteady aerodynamics within an aeroelastic CFD code such as FUN3D.

A CFD-based aeroelastic system (such as the FUN3D code) consists of the coupling of a nonlinear unsteady aerodynamic system (flow solver) with a linear structural system as depicted in Figure 1. Traditional CFD-based aeroelastic analyses are performed via iterations between the nonlinear unsteady aerodynamic system and the linear structural system. The present study focuses on the development of a linearized unsteady aerodynamic ROM (in state-space form), using the general procedure depicted in Figure 2. In this situation, the linear structural system within the CFD code is bypassed so that only the nonlinear unsteady aerodynamic system is excited. Specific modal inputs are applied to the nonlinear unsteady aerodynamic system and the generalized aerodynamic force (GAF) outputs from this solution, along with the inputs, are used in a system identification process to create the linearized unsteady aerodynamic ROM. This unsteady aerodynamic ROM is then coupled to a state-space model of the structure in order to create the aeroelastic simulation ROM. The aeroelastic simulation ROM is then used for aeroelastic analyses. For the discussions that follow, the term ROM will refer to the unsteady aerodynamic state-space model. When the unsteady aerodynamic state-space model (ROM) is connected to a state-space model of the structure within the SIMULINK environment, this system is often also referred to as a ROM. However, to avoid confusion, the SIMULINK aeroelastic system will be referred to as the aeroelastic simulation ROM.

At present, the development of CFD-based ROMs is an area of active research at several government, industry, and academic institutions [1–5]. Development of ROMs based on the Volterra theory is one of several ROM methods currently under development [6–13].

Silva and Bartels [2] introduced the development of linearized, unsteady aerodynamic

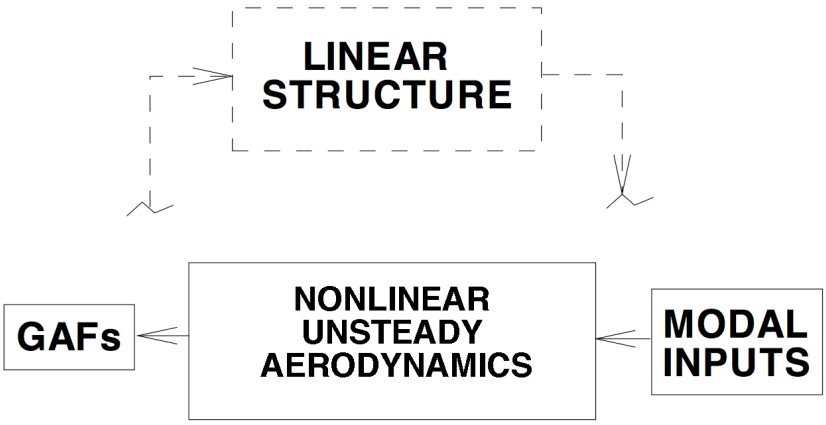

Figure 2: Generation of generalized aerodynamic forces (GAFs) used for system identification process.

state-space models for prediction of flutter and aeroelastic response using the parallelized, aeroelastic capability of the CFL3Dv6 code. The results presented provided an important validation of the various phases of the ROM development process. The Eigensystem Realization Algorithm (ERA) [14], which transforms an impulse response (one form of ROM) into state-space form (another form of ROM), was applied to the development of the aerodynamic state-space models. The ERA is part of the SOCIT (System/Observer/Controller Identification Toolbox) [15]. Flutter results for the AGARD 445.6 aeroelastic wing using the CFL3Dv6 code were presented, including computational costs [2]. Unsteady aerodynamic state-space models were generated and coupled with a structural model within a MATLAB/SIMULINK [16] environment for rapid calculation of aeroelastic responses including the prediction of flutter. Aeroelastic responses computed directly using the CFL3Dv6 code showed excellent comparison with the aeroelastic responses computed using the aeroelastic simulation ROM.

Previously, the aerodynamic impulse responses that were used to generate the unsteady aerodynamic state-space model were computed via the excitation of one mode at a time. For a four-mode system, these computations are not very expensive. However, for more realistic cases where the number of modes can be an order of magnitude or more larger, the one-mode-at-a-time method becomes prohibitively expensive. Towards the solution of this problem, Silva [17] has developed a method that enables the simultaneous excitation of the structural modes using a single CFD solution, independent of the number of structural modes. This new development greatly reduces the cost of identifying the aerodynamic impulse responses from the CFD code and thus results in the rapid development of unsteady aerodynamic ROMs. Silva [18] has also developed a method for generating static aeroelastic solutions and matched-point aeroelastic solutions using a ROM.

This paper presents the incorporation of these recent ROM enhancements into the aeroelastic capability within the FUN3D code. The paper begins with a description of the FUN3D code and the system identification methods, followed by the recently-developed ROM creation process, including a brief description of the Walsh functions (input to the FUN3D code for system identification). Results are presented for two configurations, the Benchmark Active Controls Technology (BACT) configuration and the AGARD 445.6 aeroelastic wing configuration.

2 DESCRIPTION OF FUN3D AND SYSTEM IDENTIFICATION METHODS

The following subsections describe the parallelized, aeroelastic version of the unstructured mesh solver FUN3D code, the phases of the recently-improved ROM development process, a brief description of the Walsh functions used for simultaneous excitation of the CFD unsteady aerodynamic system, and a brief description of the error minimization process.

2.1 FUN3D Code

The unstructured mesh solver used for this study is FUN3D [19]. Within the code, the unsteady Navier-Stokes equations are discretized over the median dual volume surrounding each mesh point, balancing the time rate of change of the averaged conserved variables in each dual volume with the flux of mass, momentum and energy through the instantaneous surface of the control volume. Additional details regarding the aeroelastic capability within the FUN3D code can be found in the references [20].

Because the CFD and computational structural mechanics (CSM) meshes usually do not match at the boundary interface where the grids are defined, CFD/CSM coupling requires a surface spline interpolation between the two domains. The interpolation of CSM mode shapes to CFD surface grid points is done as a preprocessing step. Modal deflections at the CFD surface grids are first generated. Mode shape displacements located at CFD surface grid points are used in the integration of the generalized modal forces and in the computation of the deflection of the deformed surface. The final surface deformation at each time step is a linear superposition of all the modal deflections.

2.2 System Identification Method

In structural dynamics, the realization of discrete-time state-space models that describe the modal dynamics of a structure has been enabled by the development of algorithms such as the Eigensystem Realization Algorithm (ERA) [14] and the Observer Kalman Identification (OKID) [21] Algorithm. These algorithms perform state-space realizations by using the Markov parameters (discrete-time impulse responses) of the systems of interest. These algorithms have been combined into one package known as the System/Observer/Controller Identification Toolbox (SOCIT) developed at NASA Langley Research Center.

There are several algorithms within the SOCIT that are used for the development of unsteady aerodynamic discrete-time state-space models. The PULSE algorithm is used to extract individual input/output impulse responses from simultaneous input/output responses. For a four-input/four-output system, simultaneous excitation of all four inputs

yields four output responses. The PULSE algorithm is used to extract the individual sixteen (four times four) impulse responses that associate the response in each of the outputs due to each of the inputs. Once the individual sixteen impulse responses are available, they are then processed via the Eigensystem Realization Algorithm (ERA) in order to transform the sixteen individual impulse responses into a four-input/four-output, discrete-time, state-space model. A brief summary of the basis of this algorithm follows.

A finite dimensional, discrete-time, linear, time-invariant dynamical system has the state-variable equations

$$x(k+1) = Ax(k) + Bu(k) \tag{1}$$

$$y(k) = Cx(k) + Du(k) \tag{2}$$

where x is an n-dimensional state vector, u an m-dimensional control input, and y a p-dimensional output or measurement vector with k being the discrete time index. The transition matrix, A, characterizes the dynamics of the system. The goal of system realization is to generate constant matrices (A, B, C, D) such that the output responses of a given system due to a particular set of inputs is reproduced by the discrete-time state-space system described above.

For the system of Eqs. (1) and (2), the time-domain values of the discrete-time impulse responses of the system are also known as the Markov parameters and are defined as

$$Y(k) = CA^{k-1}B + D \tag{3}$$

with A an (n x n) matrix, B an (n x m) matrix, C a (p x n) matrix, and D an (p x m) matrix. The ERA algorithm begins by defining the generalized Hankel matrix consisting of the discrete-time impulse responses for all input/output combinations. The algorithm then uses the singular value decomposition (SVD) to compute the A, B, C, and D matrices.

In this fashion, the ERA is applied to unsteady aerodynamic impulse responses to construct unsteady aerodynamic state-space models.

2.3 Simultaneous Excitation Input Functions

Clearly, the nonlinear unsteady aerodynamic responses of a flexible vehicle comprise a multi-input/multi-output (MIMO) system with respect to the modal inputs and generalized aerodynamic outputs. In the situation where the goal is the simultaneous excitation of a such a MIMO system, system identification techniques [23–25] dictate that the nature of the input functions used to excite the system must be properly defined if accurate input/output models of the system are to be generated. The most important point to keep in mind when defining these input functions is that these functions need to be different, in some sense, from each other. This makes sense since, if the excitation inputs are identical and they are applied simultaneously, it becomes practically impossible for any system identification algorithm to relate the effects of one input on a given output. This, in turn, makes it practically impossible for that algorithm to extract the individual impulse responses for each input/output pair. As has already been well established, the individual impulse responses for each input/output pair are necessary ingredients towards the development of state-space models.

With respect to unsteady aerodynamic MIMO systems, these individual impulse responses correspond to time-domain generalized aerodynamic forces (GAFs), critical to

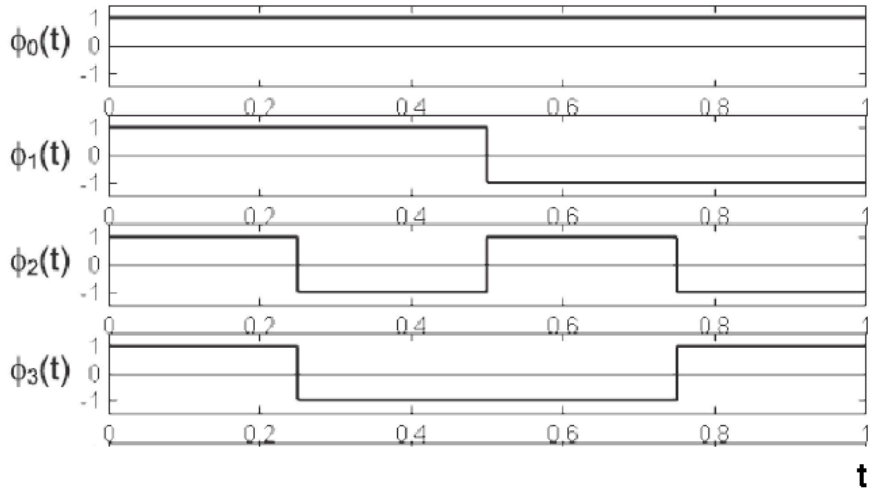

Figure 3: Walsh functions.

understanding unsteady aerodynamic behavior. The Fourier-transformed version of these GAFs are the frequency-domain GAFs which provide an important link to more traditional frequency-domain-based unsteady aerodynamic analyses.

Referring back to the input functions used to excite the MIMO system, the question is how different should these input functions be from each other and how can we quantify a level of difference between them? Since orthogonality (linear independence) is the most precise mathematical method for guaranteeing the difference between signals, recent developments focus on the application of families of orthogonal functions as candidate input functions. Using orthogonal functions directly provides a mathematical guarantee that the input functions are as different from each other as mathematically possible. These orthogonal input functions can be considered optimal input functions for the identification of a MIMO system.

In a previous paper [17], four families of functions were investigated towards the efficient identification of a CFD-based unsteady aerodynamic state-space model. For the present paper, the Walsh family of orthogonal functions [26] were used, shown in Figure 3 for four modes. These functions are orthogonal and therefore provide a benefit in the system identification process as discussed above. Also, this family of functions consist of a combination of step functions, which have been shown to be well-suited for the identification of CFD-based unsteady aerodynamic ROMs.

3 IMPROVED ROM DEVELOPMENT PROCESSES

The original ROM development process consisted of the excitation of one structural mode at a time per CFD solution. That is clearly not practical for realistic configurations with a large number of modes. As mentioned above, an improved method was recently developed and is described below.

An outline of the improved simultaneous modal excitation ROM development process with the recent enhancements is as follows:

1. Generate the number of functions (from a selected family of orthogonal functions) that corresponds to the number of structural modes;

2. Apply the generated input functions simultaneously via one CFD execution resulting in GAF responses due to these inputs; these responses are computed directly from the restart of a steady rigid CFD solution (not about a particular dynamic pressure);

3. Using the simultaneous input/output responses, identify the individual impulse responses using the PULSE algorithm (within SOCIT);

4. Transform the individual impulse responses generated in Step 3 into an unsteady aerodynamic state-space system using the ERA (within SOCIT);

5. Evaluate/validate the state-space models generated in Step 4 via comparison with CFD results (i.e., ROM results vs. full CFD solution results);

A schematic of steps 1-4 of the improved process outlined above is presented as Figure 4. Using modal information (generalized mass, frequencies, and dampings), a state-space model of the structure is generated. This state-space model of the structure is referred to as the structural state-space ROM (Figure 5). Once an unsteady aerodynamic ROM and a structural state-space ROM have been generated, they are combined to form an aeroelastic simulation ROM (see Figure 6).

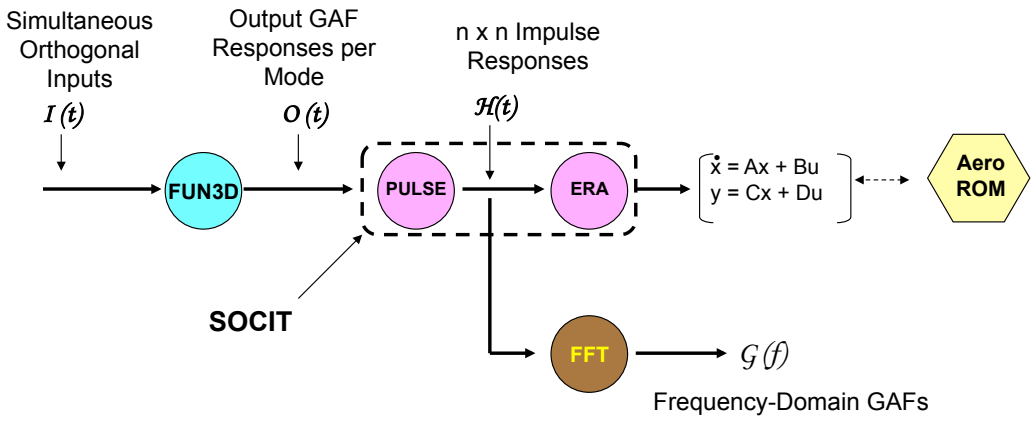

Figure 4: Improved process for generation of an unsteady aerodynamic ROM (Steps 1-4).

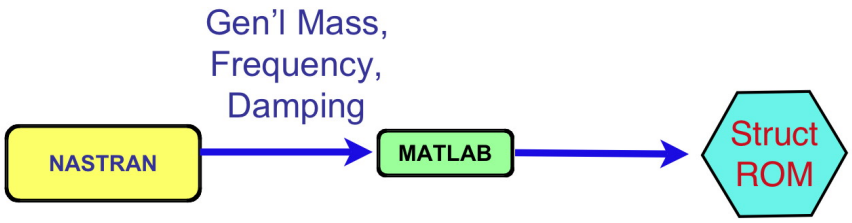

Figure 5: Process for generation of a structural state-space ROM.

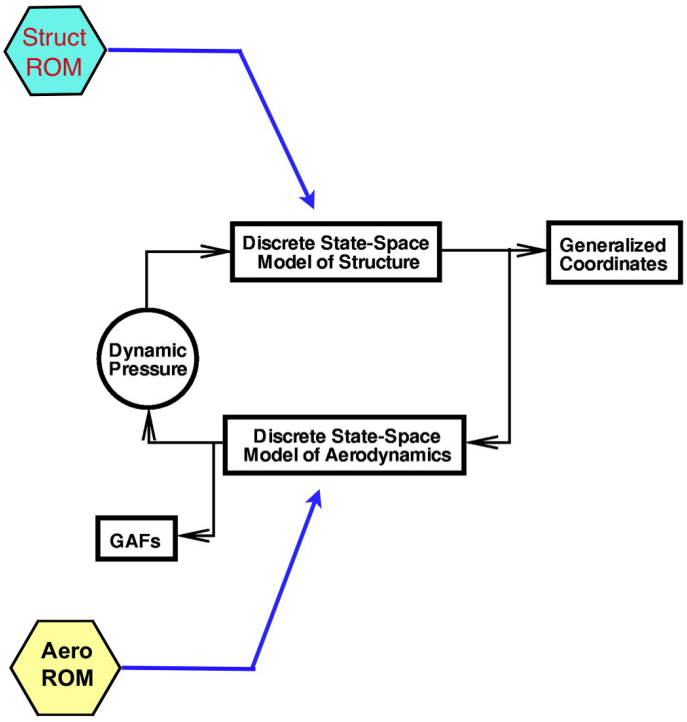

Figure 6: Process for generation of an aeroelastic simulation ROM consisting of an unsteady aerodynamic ROM and a structural state-space ROM.

An important difference between the original ROM process and the improved ROM process is stated in step (2) of the outline above. For the original ROM process, if a static aeroelastic condition existed, then a ROM was generated about a selected static aeroelastic condition. So a static aeroelastic condition of interest was defined (typically based on a dynamic pressure) and that static aeroelastic condition was computed using the CFD code as a restart from a converged steady, rigid solution. Once a converged static aeroelastic solution was obtained, the ROM process was applied about that condition. This implies that the resultant ROM is, of course, limited in some sense to the neighborhood of that static aeroelastic condition. Moving too far away from that condition could result in loss of accuracy.

The reason ROMs were generated in this fashion was because no method had been defined to enable the computation of a static aeroelastic solution using a ROM. Any ROMs generated in this fashion were, therefore, limited to the prediction of dynamic responses about a static aeroelastic solution including the methods by Raveh [5] and by Kim et al [4]. The improved ROM method, however, includes a method for generating a ROM directly from a steady, rigid solution. As a result, these improved ROMs can then be used to predict both static aeroelastic and dynamic solutions for any dynamic pressure. In order to capture a specific range of aeroelastic effects (previously obtained by selecting a particular dynamic pressure), the improved ROM method relies on the excitation amplitude of the orthogonal functions to excite aeroelastic effects of interest. The details of the method for using a ROM for computing both static aeroelastic and dynamic solutions is presented in another reference by the first author [18]. For the present results, all responses were computed from the restart of a steady, rigid FUN3D solution, bypassing the need (and additional computational expense) to execute a static aeroelastic solution using FUN3D.

3.1 Error Minimization

Error minimization consists of error quantification and error reduction. Error quantification is defined as the difference (error) between the full FUN3D solution due to the orthogonal input functions used (Walsh) and the unsteady aerodynamic ROM solution due to the same orthogonal input functions. This was identified in Step 5 in the previous subsection and is shown schematically in Figure 7. The outputs shown are GAF responses per mode. Within the system identification algorithms, there are parameters that can then be used to reduce the error (error reduction). These parameters include number of states and the record length of the identified pulse responses, for example. The maximum error is the largest error encountered per mode. Using the maximum error as the figure of merit, the parameters are varied until an acceptable ROM has been obtained.

4 CONFIGURATIONS

Two configurations were used for the present analyses: the Benchmark Active Controls Technology (BACT) configuration and the AGARD 445.6 aeroelastic wing. The two-dimensional viscous grid for the BACT is presented as Figure 8. This grid consists of 39,000 nodes on the 2D plane containing 39,000 hexahedral cells. The BACT unstructured hexahedral grid was generated from a 305x129x2 structured grid. The BACT aeroelastic system consists of two degrees of freedom, plunge and pitch [27].

The three-dimensional grid of the AGARD 445.6 aeroelastic wing consists of 431,000 nodes

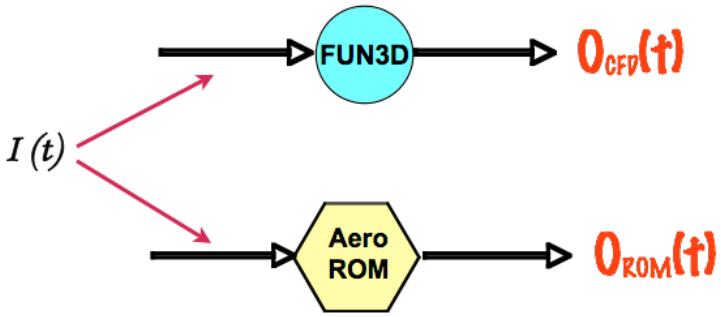

Figure 7: Error defined as difference between the FUN3D solution and the unsteady aerodynamic ROM solution due to input of orthogonal functions.

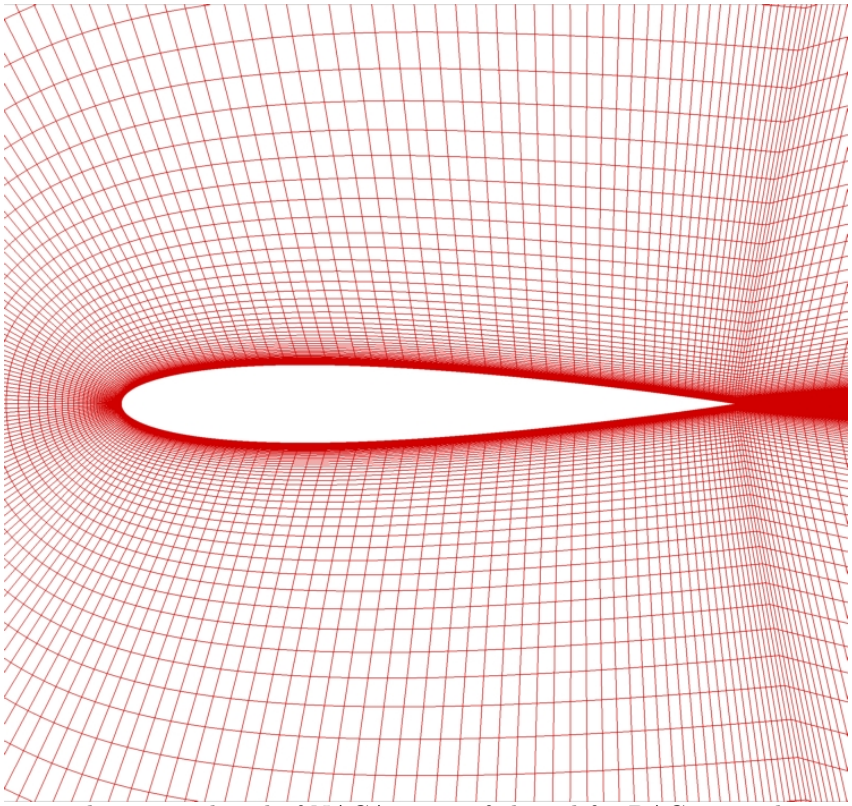

Figure 8: Two-dimensional grid of NACA0012 airfoil used for BACT aeroelastic analyses.

(2.23M tetrahedral cells) and is presented as Figure 9. The AGARD 445.6 aeroelastic wing is a frequently used configuration in the validation of aeroelastic analysis methods [28–31].

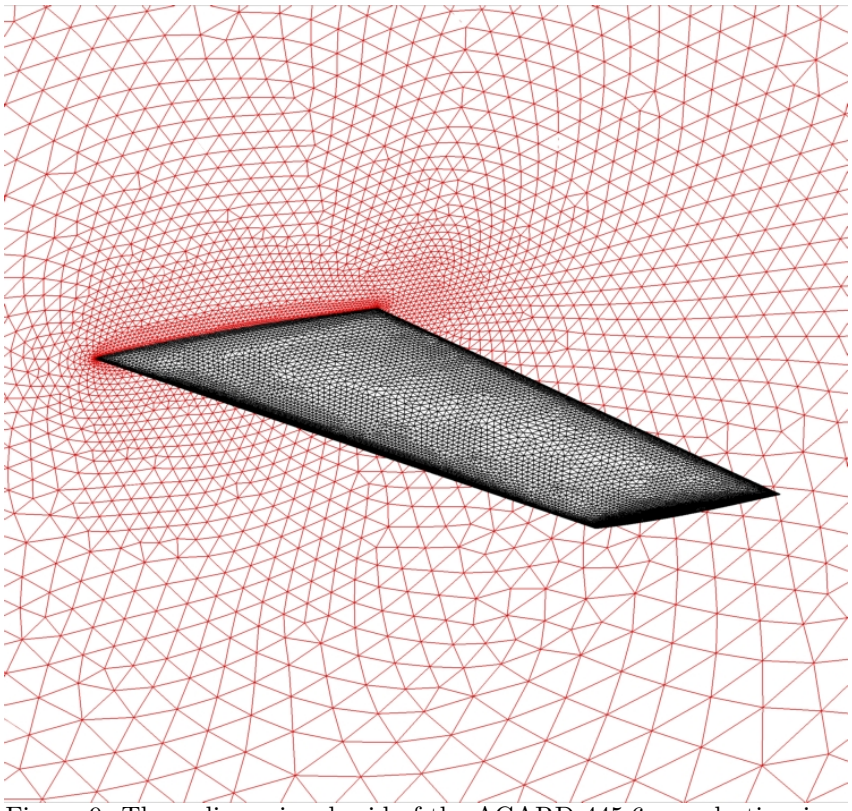

Figure 9: Three-dimensional grid of the AGARD 445.6 aeroelastic wing.

5 RESULTS

5.1 BACT, 2D, Viscous

Applying the methods described above, an unsteady aerodynamic ROM was generated for the BACT 2D viscous configuration. This is a two-degree-of-freedom problem with a plunge and a pitch mode. Therefore, two Walsh functions were generated, one per mode, and submitted simultaneously as input to the FUN3D code. This solution was generated at a Mach number of 0.51 with a non-dimensional time step of 5 and 9500 time steps.

The generalized aerodynamic force (GAF) outputs from FUN3D due to two Walsh input functions (one per mode) were used to generate a preliminary unsteady aerodynamic ROM. The error minimization process was then applied and comparisons of the FUN3D solution due to the Walsh input functions and the unsteady aerodynamic ROM solution due to the same Walsh input functions are presented as Figure 10 and Figure 11 for mode 1 and mode 2 respectively. As can be seen in Figure 12, an unsteady aerodynamic ROM was converged upon with a maximum error of 2.4 percent in the first mode. This unsteady aerodynamic ROM was then incorporated into an aeroelastic simulation ROM for subsequent aeroelastic analyses.

A comparison of the aeroelastic responses computed directly from FUN3D with those computed using the aeroelastic simulation ROM are presented in Figure 13 for the first generalized coordinate and in Figure 14 for the second generalized coordinate. These

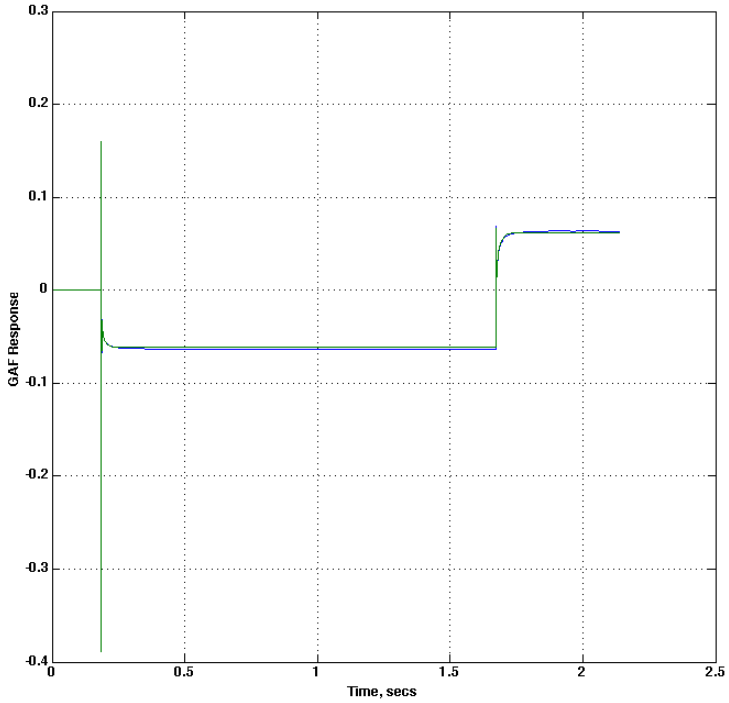

Figure 10: Comparison of FUN3D and ROM GAF responses in mode 1 due to Walsh input functions for the BACT configuration; Blue=FUN3D, Green=ROM.

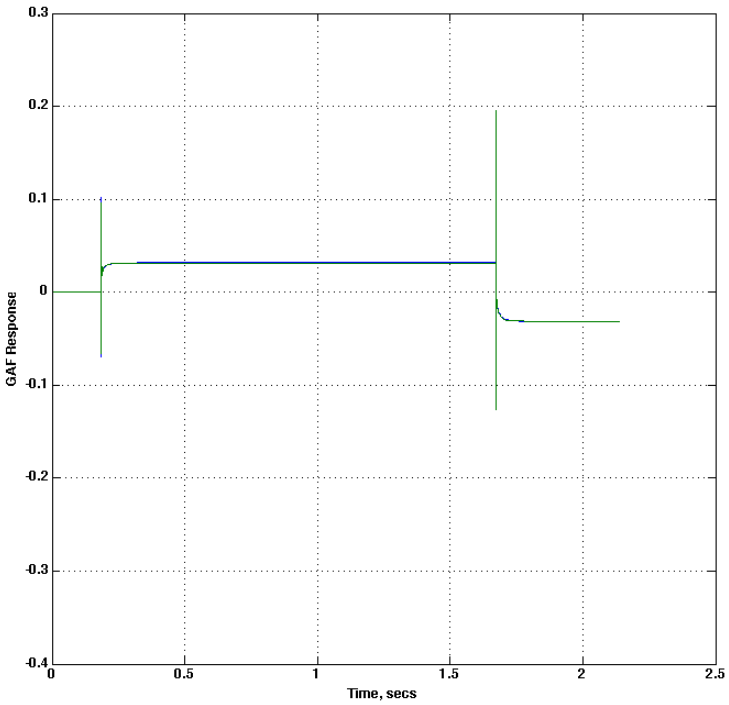

Figure 11: Comparison of FUN3D and ROM GAF responses in mode 2 due to Walsh input functions for the BACT configuration; Blue=FUN3D, Green=ROM.

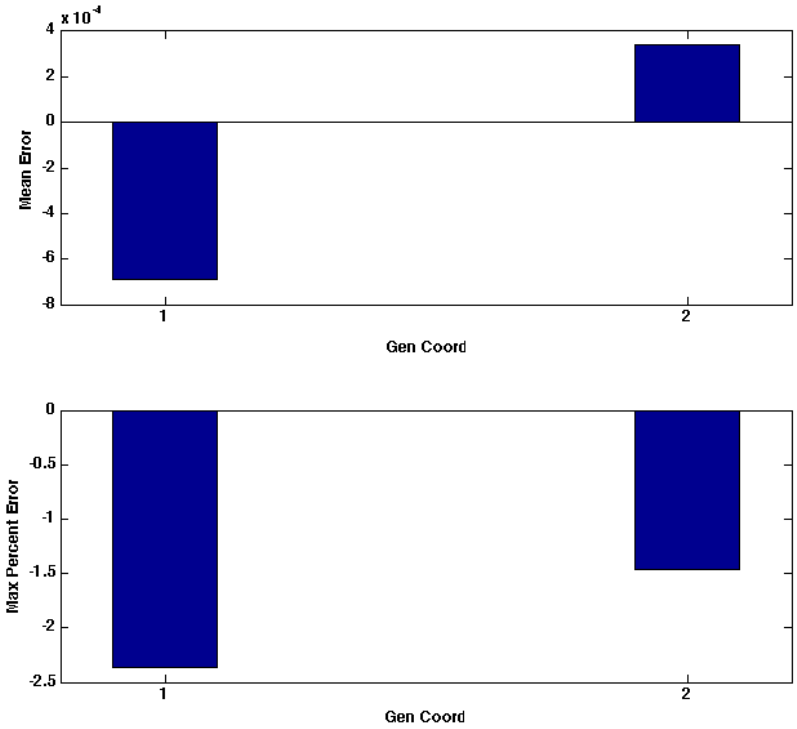

Figure 12: Mean and maximum percent error between the FUN3D solution and the ROM solution for modes 1 and 2 for the BACT configuration.

results assume a structural damping of 0.2 percent. As can be seen, the comparison is very good.

Presented in Figure 15 is the time-domain (upper plot) and frequency-domain (lower plot) aeroelastic responses for both modes of the aeroelastic simulation ROM at zero dynamic pressure. This solution is typically generated in order to verify the wind-off frequencies of the configuration which in this case correspond to 3.36 Hz for the first mode and 5.12 Hz for the second mode. Figure 16, Figure 17, and Figure 18 are similar plots for dynamic pressures of 100 psf, 140 psf, and 150 psf, respectively. As can be seen, as dynamic pressure is increased, there is a coalescence of frequencies and a corresponding decrease in the damping of the aeroelastic responses. At a dynamic pressure of 150 psf, the system is unstable, indicating that the flutter dynamic pressure for this Mach number is between 140 and 150 psf.

These ROM solutions at different dynamic pressures represent the original format for presenting aeroelastic results from an aeroelastic simulation ROM. Although these solutions are generated in seconds and flutter is captured as the dynamic pressure is varied, this solution format does not provide insight regarding the flutter mechanism itself. Therefore, a method was developed to directly generate a root locus solution that would clearly present the nature of the flutter mechanism. Presented in Figure 19 is the discrete-time (z-transform) version of the root locus for the aeroelastic simulation ROM. Most of the roots are related to the unsteady aerodynamic ROM while the dominant aeroelastic roots are closer to the origin. Figure 20 presents the root locus in terms of Frequency in Hertz as a function of Damping Ratio. As can be seen, the flutter mechanism consists of the

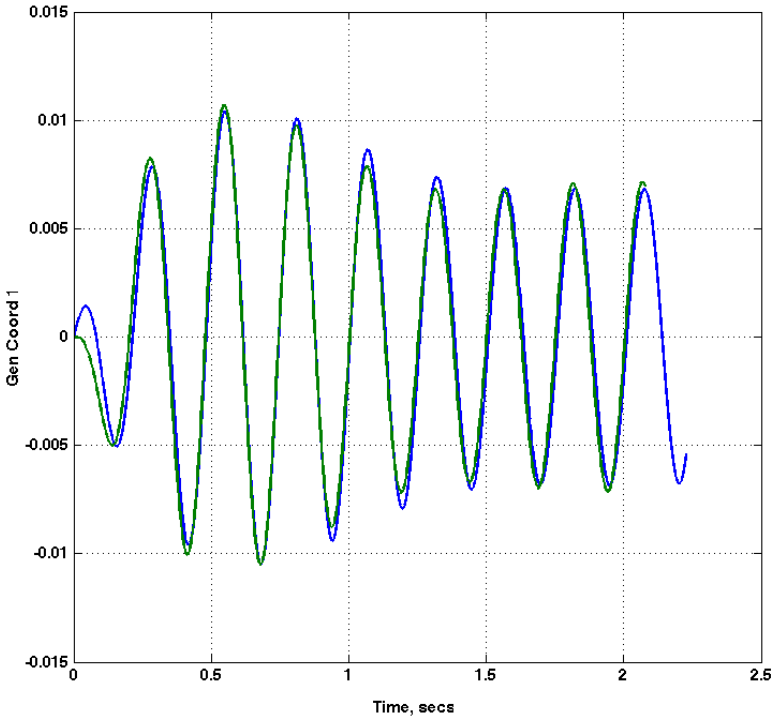

Figure 13: Comparison of aeroelastic response of the first generalized coordinate of the BACT configuration at a dynamic pressure Q=140 psf; Blue=ROM, Green=FUN3D.

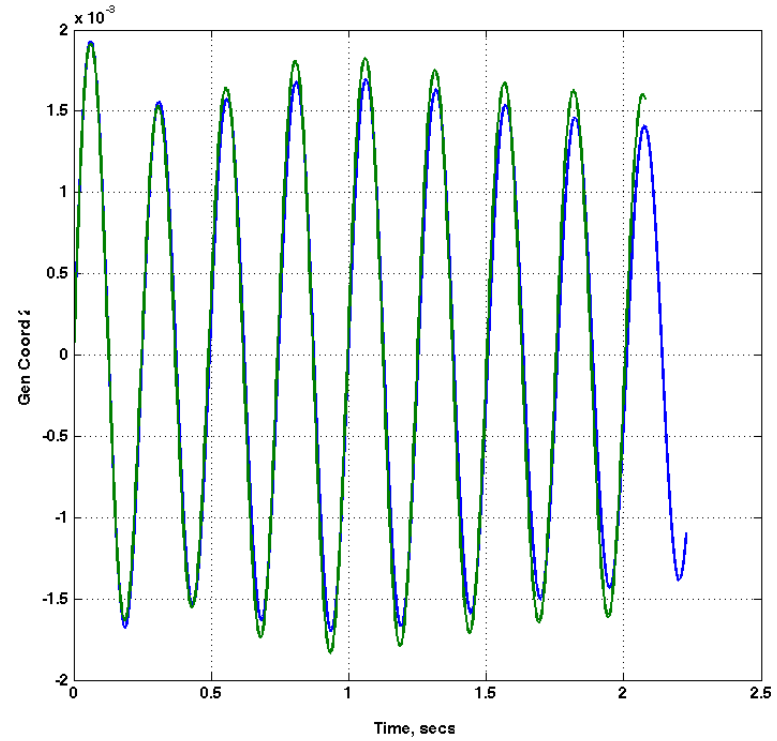

Figure 14: Comparison of aeroelastic response of the second generalized coordinate of the BACT configuration at a dynamic pressure Q=140 psf; Blue=ROM, Green=FUN3D.

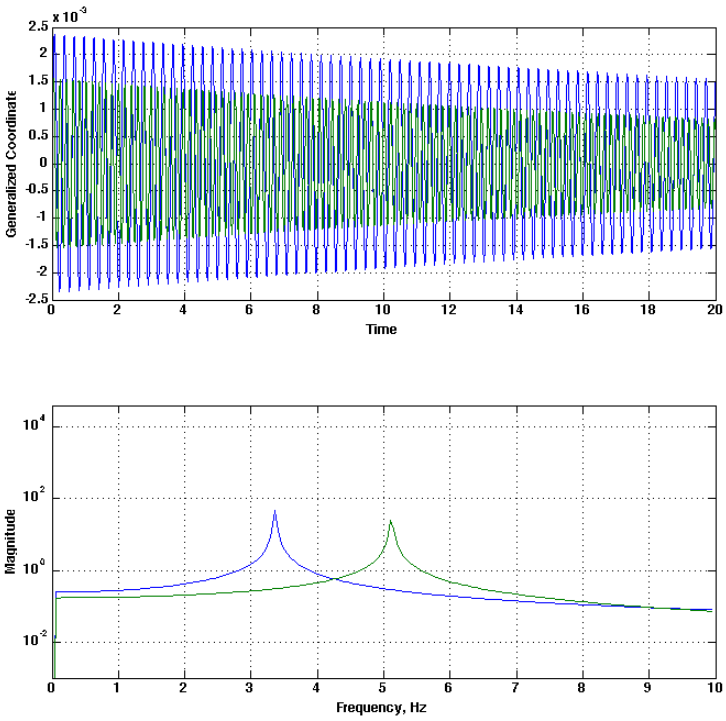

Figure 15: Time- and frequency-domain responses from the aeroelastic simulation ROM of the BACT configuration at a dynamic pressure Q=0 psf; Blue=mode 1, Green=mode2.

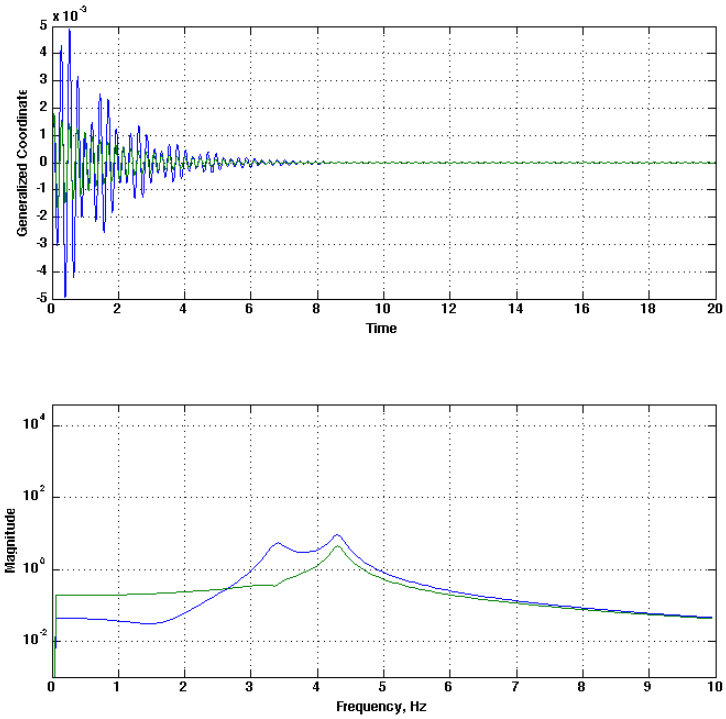

Figure 16: Time- and frequency-domain responses from the aeroelastic simulation ROM of the BACT configuration at a dynamic pressure Q=100 psf; Blue=mode 1, Green=mode2.

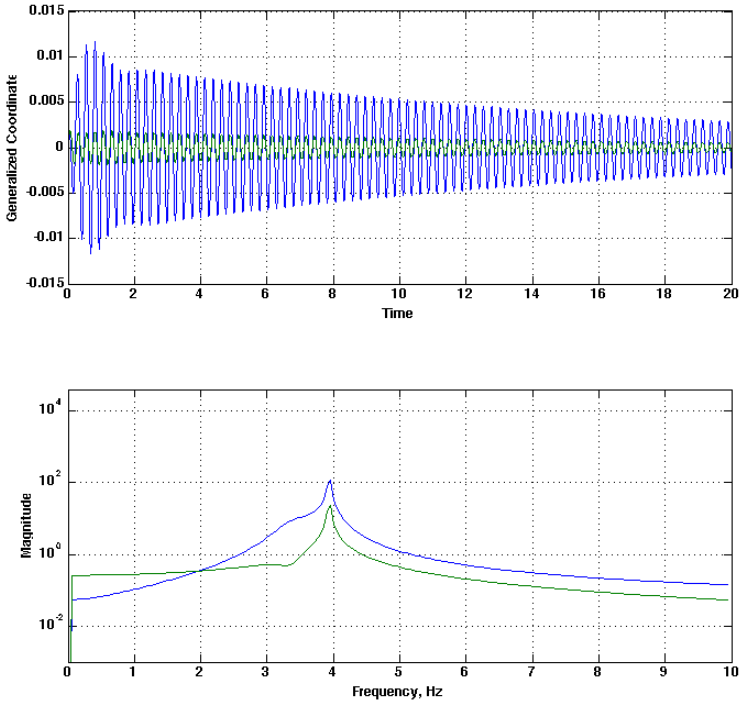

Figure 17: Time- and frequency-domain responses from the aeroelastic simulation ROM of the BACT configuration at a dynamic pressure Q=140 psf; Blue=mode 1, Green=mode2.

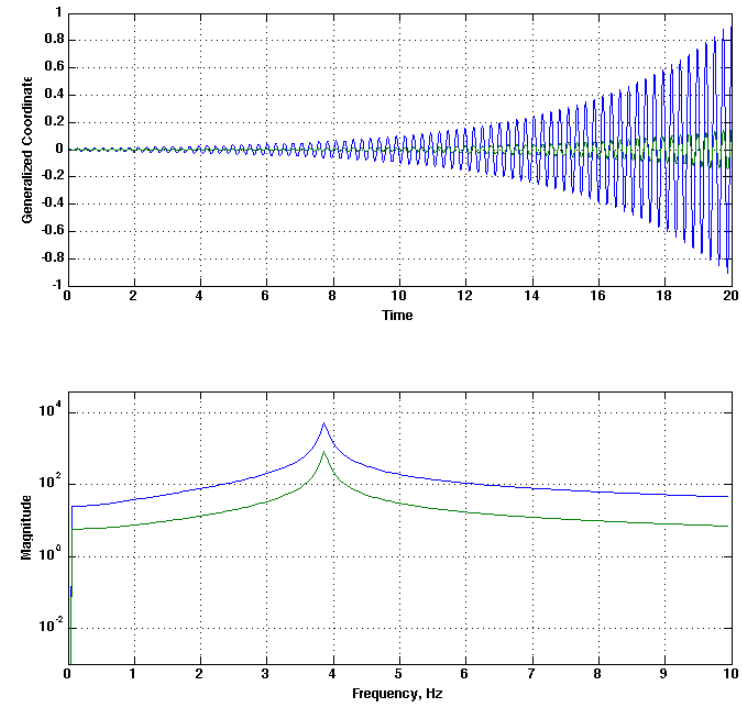

Figure 18: Time- and frequency-domain responses from the aeroelastic simulation ROM of the BACT configuration at a dynamic pressure Q=150 psf; Blue=mode 1, Green=mode2.

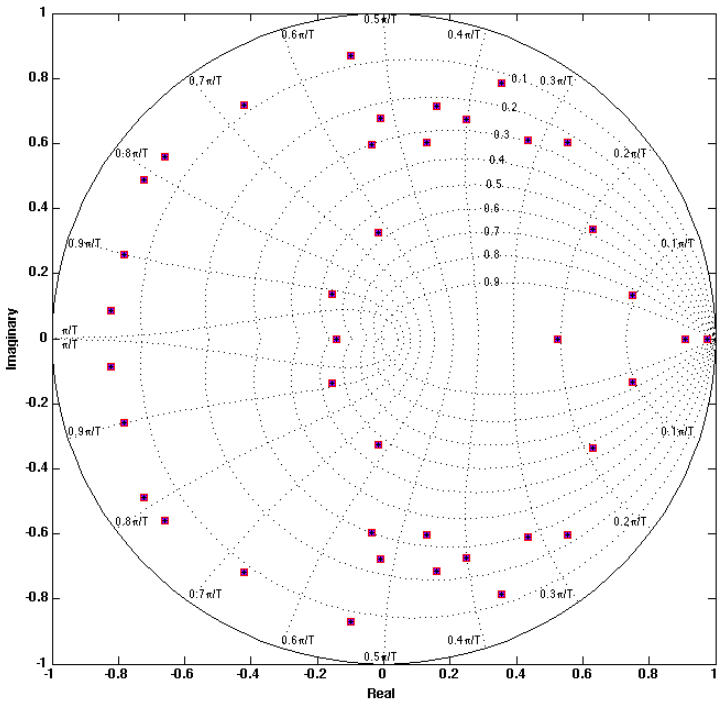

Figure 19: Discrete-time (Z-plane) mapping of unsteady aerodynamic and aeroelastic roots for the BACT configuration.

destabilization of the second mode as it couples with the first mode. Consistent with the time-domain plots, flutter occurs between 140 and 150 psf.

5.2 AGARD 445.6 Aeroelastic Wing, 3D, Inviscid

In an identical fashion to the process applied to the BACT 2D viscous configuration, an unsteady aerodynamic ROM was generated for the AGARD 445.6 aeroelastic wing. Results for this configuration were generated at a Mach number of 0.9 with a non-dimensional time step of 0.3 and 3500 time steps. For this configuration, the first four modes were used in the analysis with zero structural damping.

Presented in Figure 21, Figure 22, Figure 23, and Figure 24 are the comparisons of the FUN3D GAF solution due to the Walsh input functions and the unsteady aerodynamic ROM solution due to the same Walsh input functions for all four modes. As can be seen, the unsteady aerodynamic ROM generated has excellent correlation with the full FUN3D solution. The error is presented in Figure 25 where it can be seen that the maximum error is 0.15 percent in mode 1.

Finally, the unsteady aerodynamic ROM generated above is incorporated into an aeroelastic simulation ROM. A comparison of the aeroelastic responses computed directly from FUN3D with those computed using the aeroelastic simulation ROM are presented in Figure 26, Figure 27, Figure 28, and Figure 29 for the first, second, third, and fourth generalized coordinates respectively at a dynamic pressure Q=75 psf. As can be seen, the comparison is very good.

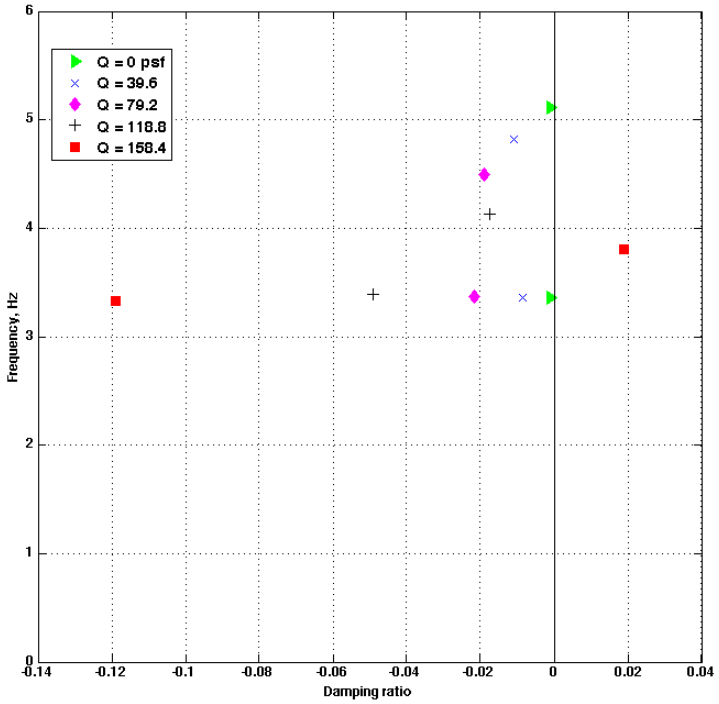

Figure 20: Root locus of aeroelastic simulation ROM of the BACT configuration presented in terms of Frequency in Hertz as a function of Damping Ratio.

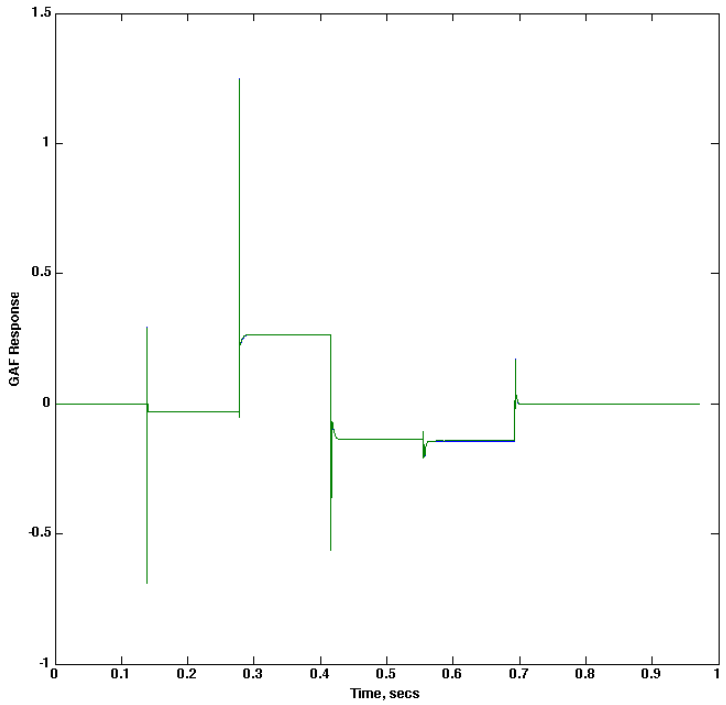

Figure 21: Comparison of FUN3D and ROM GAF responses in mode 1 due to Walsh input functions for the AGARD aeroelastic wing; Blue=FUN3D, Green=ROM.

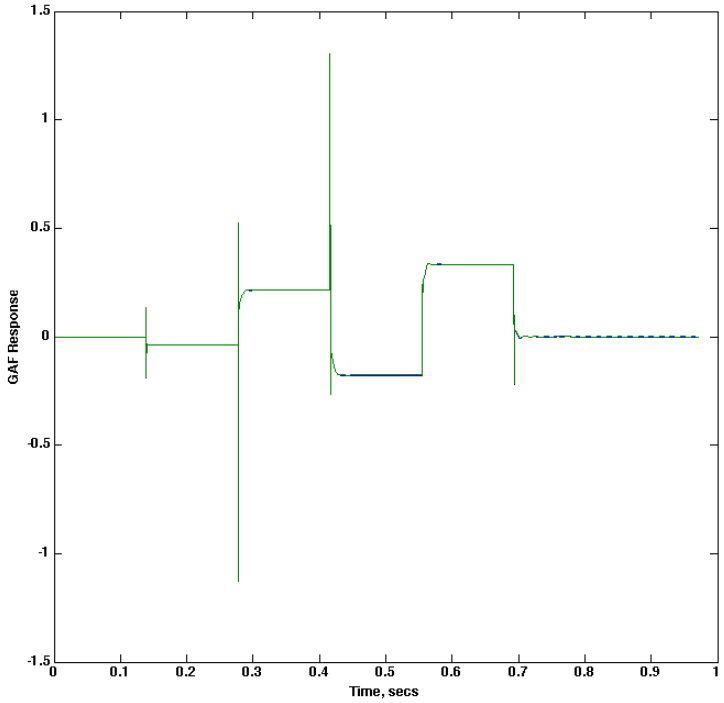

Figure 22: Comparison of FUN3D and ROM GAF responses in mode 2 due to Walsh input functions for the AGARD aeroelastic wing; Blue=FUN3D, Green=ROM.

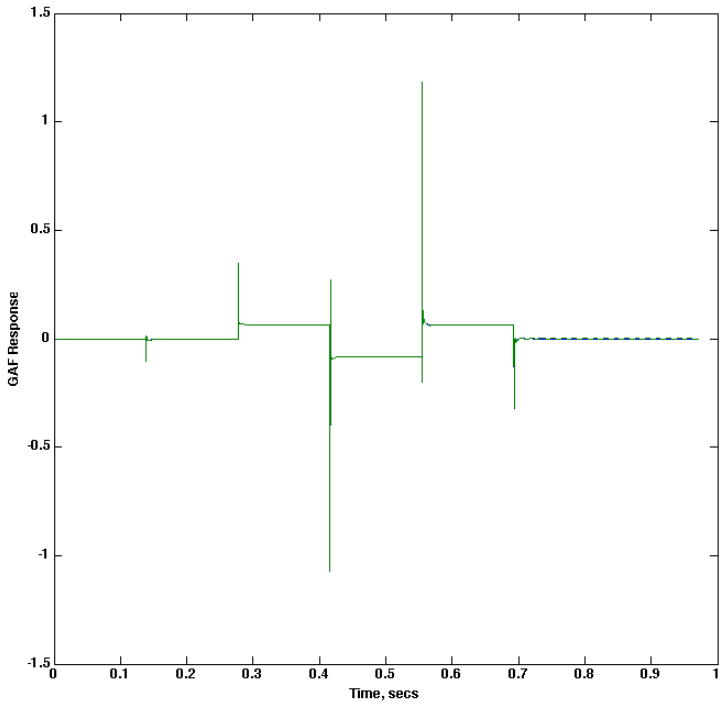

Figure 23: Comparison of FUN3D and ROM GAF responses in mode 3 due to Walsh input functions for the AGARD aeroelastic wing; Blue=FUN3D, Green=ROM.

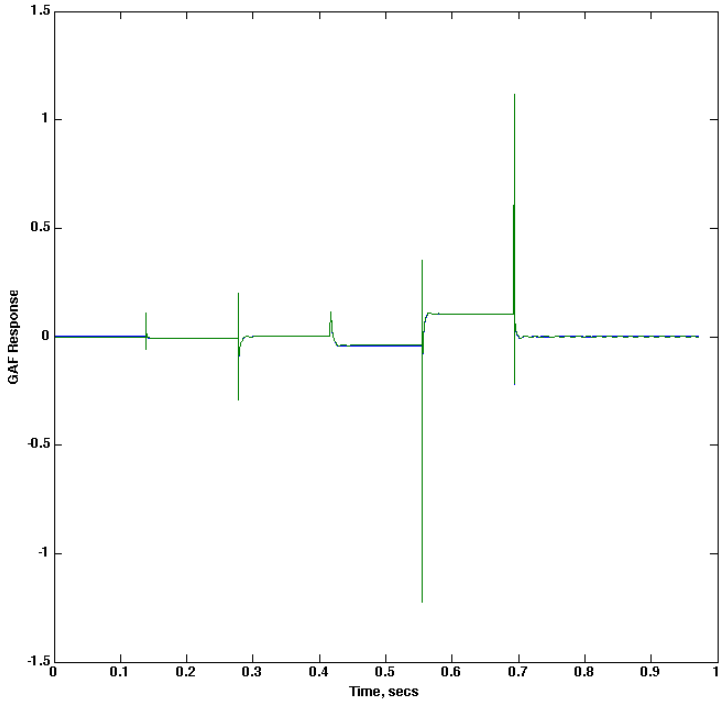

Figure 24: Comparison of FUN3D and ROM GAF responses in mode 4 due to Walsh input functions for the AGARD aeroelastic wing; Blue=FUN3D, Green=ROM.

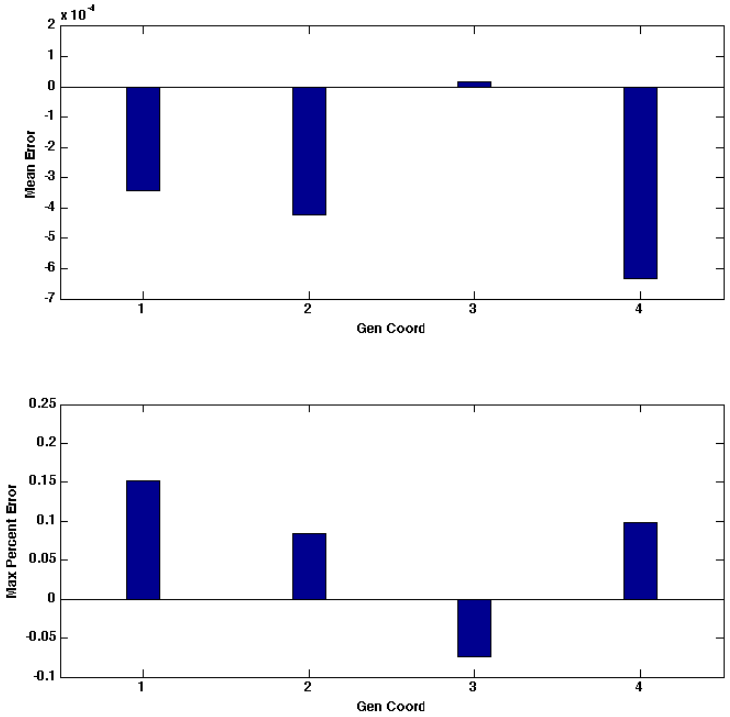

Figure 25: Mean and maximum percent error between the FUN3D solution and the ROM solution for modes 1, 2, 3, and 4 for the AGARD aeroelastic wing.

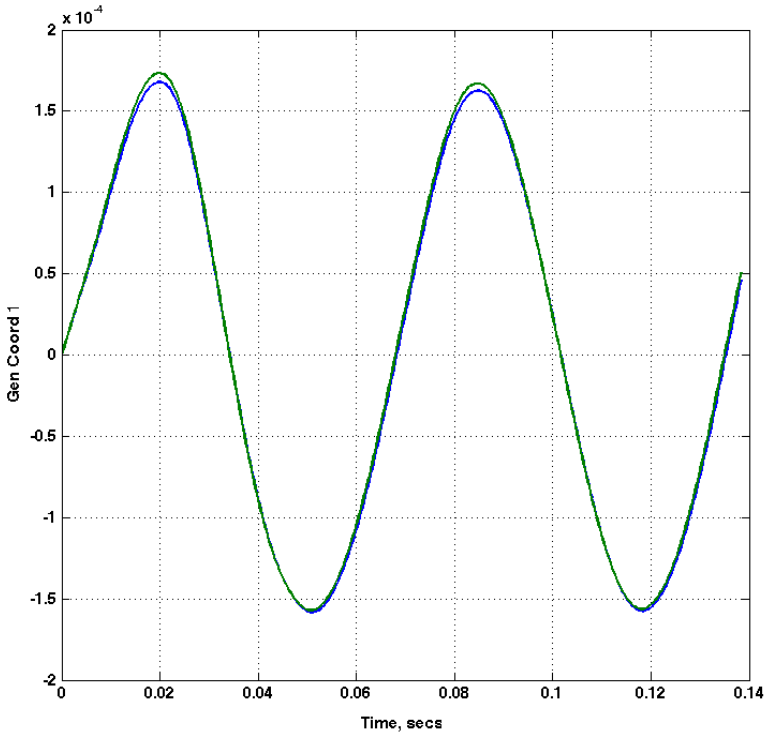

Figure 26: Comparison of aeroelastic response of the first generalized coordinate for the AGARD aeroelastic wing at a dynamic pressure Q=75 psf; Blue=ROM, Green=FUN3D.

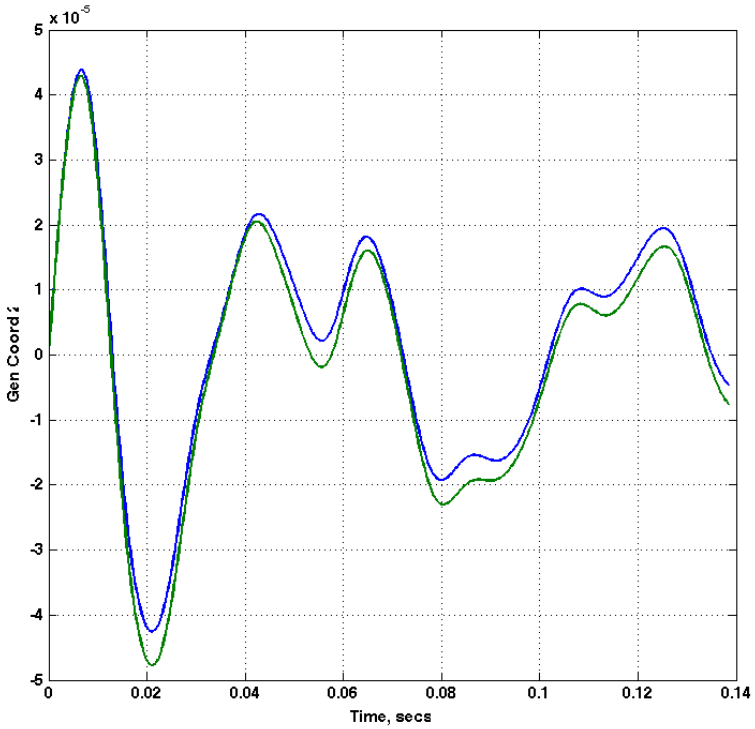

Figure 27: Comparison of aeroelastic response of the second generalized coordinate for the AGARD aeroelastic wing at a dynamic pressure Q=75 psf; Blue=ROM, Green=FUN3D.

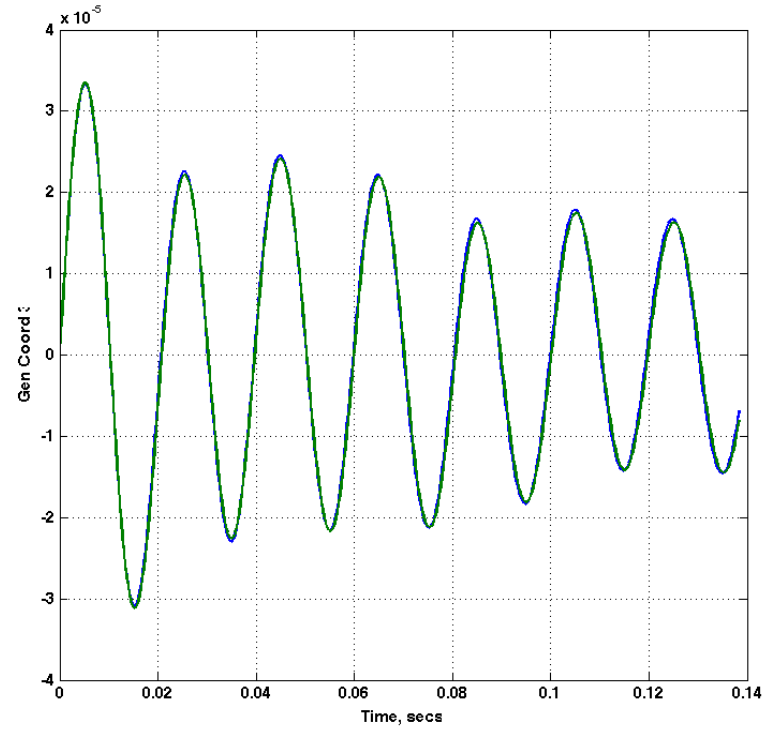

Figure 28: Comparison of aeroelastic response of the third generalized coordinate for the AGARD aeroelastic wing at a dynamic pressure Q=75 psf; Blue=ROM, Green=FUN3D.

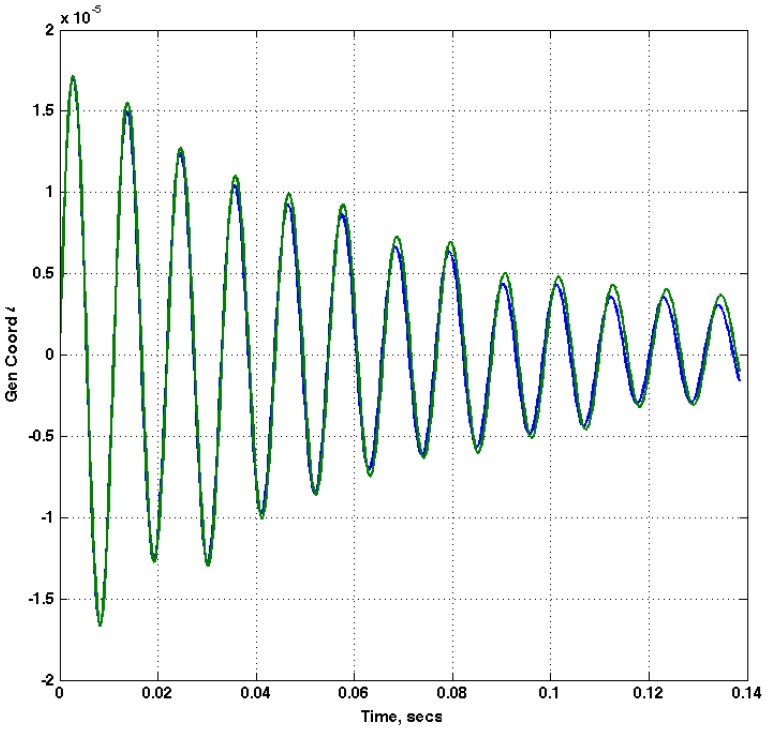

Figure 29: Comparison of aeroelastic response of the fourth generalized coordinate for the AGARD aeroelastic wing at a dynamic pressure Q=75 psf; Blue=ROM, Green=FUN3D.

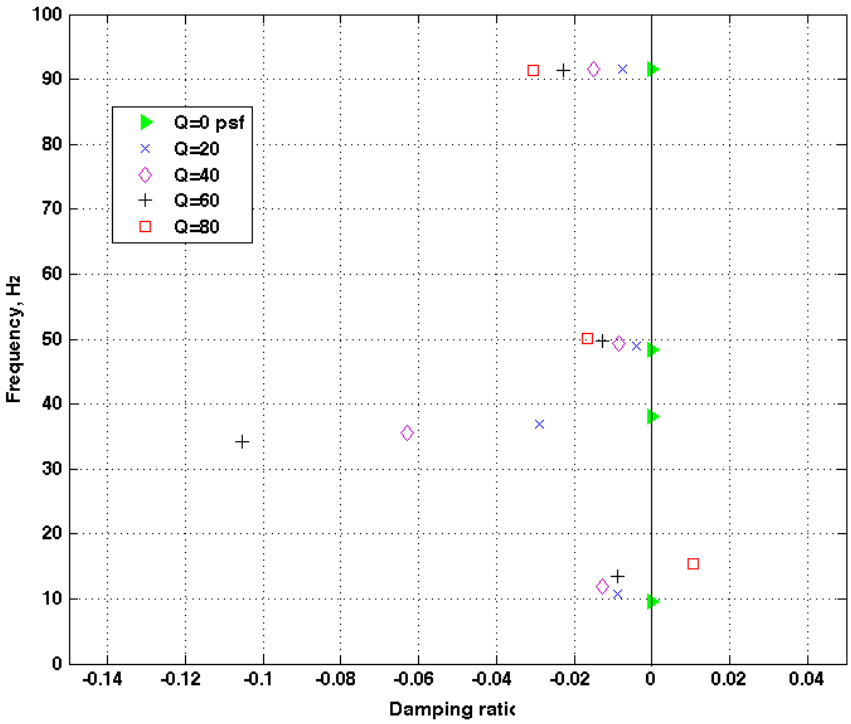

Figure 30: Root locus of aeroelastic simulation ROM presented in terms of Frequency in Hertz as a function of Damping Ratio for the AGARD aeroelastic wing.

The root locus method is then applied resulting in Figure 30. The root locus for this configuration at this condition indicates a destabilization of the first mode as the flutter mechanism. The flutter dynamic pressure is indicated to be between 60 and 80 psf, in good agreement with published results.

6 CONCLUDING REMARKS

An improved method for generating unsteady aerodynamic state-space reduced-order models (ROMs) was implemented into the aeroelastic capability of the FUN3D code. This capability enables the simultaneous excitation of an unsteady aerodynamic FUN3D model, consisting of any number of modes, with a single FUN3D execution. This is achieved by the introduction of orthogonal functions as the input excitations to the system. Comparisons of generalized aerodynamic forces (GAFs) were presented for the Walsh family of functions. An error minimization technique was introduced that aids in the creation of minimal-error unsteady aerodynamic ROMs. Aeroelastic results were presented in root locus form using the aeroelastic simulation ROMs.

7 REFERENCES

[1] Silva, W. A., "Identification of Nonlinear Aeroelastic Systems Based on the Volterra Theory: Progress and Opportunities," *Journal of Nonlinear Dynamics*, Vol. 39, Jan. 2005.

[2] Silva, W. A. and Bartels, R. E., "Development of Reduced-Order Models for Aeroelastic Analysis and Flutter Prediction Using the CFL3Dv6.0 Code," *Journal of Fluids and Structures*, No. 19, 2004, pp. 729–745.

[3] Beran, P. S. and Silva, W. A., "Reduced-Order Modeling: New Approaches for Computational Physics," *Presented at the 39th AIAA Aerospace Sciences Meeting, 8-11 January 2001, Reno,NV*, January 2001.

[4] Kim, T., Hong, M., Bhatia, K. G., and SenGupta, G., "Aeroelastic Model Reduction for Affordable Computational Fluid Dynamics-Based Flutter Analysis," *AIAA Journal*, Vol. 43, 2005, pp. 2487–2495.

[5] Raveh, D. E., "Identification of Computational-Fluid-Dynamic Based Unsteady Aerodynamic Models for Aeroelastic Analysis," *Journal of Aircraft*, Vol. 41, June 2004, pp. 620–632.

[6] Silva, W. A., Beran, P. S., Cesnik, C. E. S., Guendel, R. E., Kurdila, A., Prazenica, R. J., Librescu, L., Marzocca, P., and Raveh, D., "Reduced-Order Modeling: Cooperative Research and Development at the NASA Langley Research Center," *CEAS/AIAA/ICASE/NASA International Forum on Aeroelasticity and Structural Dynamics*, June 2001.

[7] Silva, W. A., "Reduced-Order Models Based on Linear and Nonlinear Aerodynamic Impulse Responses," *CEAS/AIAA/ICASE/NASA International Forum on Aeroelasticity and Structural Dynamics*, June 1999.

[8] Silva, W. A., *Discrete-Time Linear and Nonlinear Aerodynamic Impulse Responses for Efficient CFD Analyses*, Ph.D. thesis, College of William & Mary, December 1997.

[9] Silva, W. A., "Application of Nonlinear Systems Theory to Transonic Unsteady Aerodynamic Responses," *Journal of Aircraft*, Vol. 30, 1993, pp. 660–668.

[10] Raveh, D. E., Levy, Y., and Karpel, M., "Aircraft Aeroelastic Analysis and Design Using CFD-Based Unsteady Loads," *41st Structures, Structural Dynamics, and Materials Conference*, No. 2000-1325, Atlanta, GA, April 2000.

[11] Balajewicz, M., Nitzche, F., and Feszty, D., "Reduced Order Modeling of Nonlinear Transonic Aerodynamics Using a Pruned Volterra Series," *Proceedings of the 50th AIAA/ASME/ASCE/AHS/ASC Structures, Structural Dynamics, and Materials Conference*, Palm Springs, CA, May 2009, AIAA-2009-2319.

[12] Omran, A. and Newman, B., "Piecewise Global Volterra Nonlinear Modeling and Characterization for Aircraft Dynamics," *Journal of Guidance, Control, and Dynamics*, Vol. 32, No. 3, 2009, pp. 749–759.

[13] Milanese, A. and Marzocca, P., "Volterra Kernels Identification Using Continuous Time Impulses Applied to Nonlinear Aeroelastic Problems," *presented at the 50th AIAA/ASME/ASCE/AHS/ASC Structures, Structural Dynamics, and Materials Conference, 4-7 May 2009, Palm Springs, CA*, 4-7 May 2009.

[14] Juang, J.-N. and Pappa, R. S., "An Eigensystem Realization Algorithm for Modal Parameter Identification and Model Reduction," *Journal of Guidance, Control, and Dynamics*, Vol. 8, 1985, pp. 620–627.

[15] Juang, J.-N., *Applied System Identification*, Prentice-Hall PTR, 1994.

[16] "Registered Product of the MathWorks, Inc." .

[17] Silva, W. A., "Simultaneous Excitation of Multiple-Input/Multiple-Output CFD-Based Unsteady Aerodynamic Systems," *Journal of Aircraft*, Vol. 45, No. 4, July-August 2008, pp. 1267–1274.

[18] Silva, W. A., "Recent Enhancements to the Development of CFD-Based Aeroelastic Reduced Order Models," *48th AIAA/ASME/ASCE/AHS/ASC Structures, Structural Dynamics, and Materials Conference*, No. AIAA Paper No. 2007-2051, Honolulu, HI, April 23-26 2007.

[19] Anderson, W. K. and Bonhaus, D. L., "An Implicit Upwind Algorithm for Computing Turbulent Flows on Unstructured Grids," *Computers and Fluids*, Vol. 23, No. 1, 1994, pp. 1–21.

[20] Biedron, R. T. and Thomas, J. L., "Recent Enhancements to the FUN3D Flow Solver for Moving Mesh Applications," *47th AIAA Aerospace Sciences Meeting, Orlando, FL*, January 2009.

[21] Juang, J.-N., Phan, M., Horta, L. G., and Longman, R. W., "Identification of Observer/Kalman Filter Markov Parameters: Theory and Experiments," *Journal of Guidance, Control, and Dynamics*, Vol. 16, 1993, pp. 320–329.

[22] Silva, W. A., "Simultaneous Excitation of Multiple-Input Multiple-Output CFD-Based Unsteady Aerodynamic Systems," *48th AIAA/ASME/ASCE/AHS/ASC Structures, Structural Dynamics, and Materials Conference*, No. AIAA Paper No. 2007-1988, Honolulu, HI, April 23-26 2007.

[23] Eykhoff, P., *System Identification: Parameter and State Identification*, Wiley Publishers, 1974.

[24] Ljung, L., *System Identification: Theory for the User*, Prentice-Hall Publishers, 1999.

[25] Zhu, Y., *Multivariable System Identification for Process Control*, Pergamon Publishers, 2001.

[26] Pacheco, R. P. and V. Steffen, J., "Using Orthogonal Functions for Identification and Sensitivity Analysis of Mechanical Systems," *Journal of Vibration and Control*, Vol. 8, June 2002, pp. 993–1021.

[27] Scott, R. C., Hoadley, S. T., Wieseman, C. D., and Durham, M. H., "The Benchmark Active Controls Technology Model Aerodynamic Data," *35th Aerospace Sciences Meeting and Exhibit*, Reno, NV, 1997.

[28] Gordnier, R. E. and Melville, R. B., "Transonic Flutter Simulations Using an Implicit Aeroelastic Solver," *AIAA Journal of Aircraft*, Vol. 37, 2000, pp. 872–879.

[29] Gupta, K. K., Voelker, L. S., Bach, C., Doyle, T., and Hahn, E., "CFD-Based Aeroelastic Analysis of the X-43 Hypersonic Flight Vehicle," *Proceedings of the 39th Aerospace Sciences Meeting and Exhibit*, No. 2001-0712, Reno, CA, Jan. 2001.

[30] Lee-Rausch, E. M. and Batina, J. T., "Wing Flutter Computations Using an Aerodynamic Model Based on the Navier-Stokes Equations," *Journal of Aircraft*, Vol. 33, 1993, pp. 1139–1148.

[31] E. C. Yates, J., Land, N. S., and J. T. Foughner, J., "Measured and Calculated Subsonic and Transonic Flutter Characteristics of a 45-degree Swept-Back Wing Planform in Air and in Freon-12 in the Langley Transonic Dynamics Tunnel," Tech. rep., NASA, TN D-1616, 1963.